frontiers in Earth Science

ORIGINAL RESEARCH
published: 17 March 2022
doi: 10.3389/feart.2022.844566

Water-Rich Soft Soil Freezing Method Combined With Steel Sleeve Receiving-Shield Technology Field Test Research

Y. Mei[1], *Y. Y. Liu*[1]*, *X. Yan*[1], *C. Liang*[2] *and J. T. Zhu*[2]

[1]School of Civil Engineering, Xi'an University of Architecture and Technology, Xi'an, China, [2]China Railway Seventh Bureau Group Third Engineering Co., Ltd., Xi'an, China

The initiation and reception of shields are major risk events for shield construction in water-rich and weak strata. Although the freezing method and the steel sleeve method receiving-shield tunneling technologies both have engineering applications, the environmental safety control effect cannot meet the construction requirements of water-rich soft soil. Considering the shield construction of a typical soft soil layer in Suzhou, China, as a research target, the applicability and safety of the freezing method combined with steel sleeve receiving-shield technology in water-rich soft soil were evaluated based on a field test system. The test results show that, during soil freezing, the temperature change trend of each measuring point in the temperature measuring hole is roughly the same. The freezing process can be divided into five typical stages. The closer the active freezing period of the water-rich soft soil is to the inside of the frozen-soil curtain, the faster the development rate of the frozen wall. The soil cooling gradient increased with an increase in the radial depth. After freezing the curtain circle, the soil frost heave significantly accelerated until the frost heave amount peaked. During the construction process, special attention should be paid to the change in the value of the soil settlement during each stage change to prevent sudden changes in soil displacement. The freezing method, combined with steel sleeve receiving-shield technology, can effectively reduce the environmental disturbance caused by shield construction in water-rich soft soil.

Keywords: water-rich soft soil, horizontal freeze, steel sleeve, freezing temperature field, ground subsidence

OPEN ACCESS

Edited by:
Jinyang Fan,
Chongqing University, China

Reviewed by:
Caihui Zhu,
Xi'an University of Technology, China
Shu Yu,
China Institute of Water Resources and Hydropower Research, China

***Correspondence:**
Y. Y. Liu
liuyuanying@xauat.edu.cn

Specialty section:
This article was submitted to Geohazards and Georisks, a section of the journal Frontiers in Earth Science

Received: *28 December 2021*
Accepted: *10 February 2022*
Published: *17 March 2022*

Citation:
Mei Y, Liu YY, Yan X, Liang C and Zhu J (2022) Water-Rich Soft Soil Freezing Method Combined With Steel Sleeve Receiving-Shield Technology Field Test Research. Front. Earth Sci. 10:844566. doi: 10.3389/feart.2022.844566

1 INTRODUCTION

The initiation and reception of shields is one of the major risk events for shield construction in water-rich and weak strata. Although the freezing method and the steel sleeve method of receiving-shield tunneling technology have engineering applications (Ding et al., 2017; Hu J. et al., 2017; Zhao et al., 2017; Li X. et al., 2021; Ren et al., 2019; Dong et al., 2021; Li et al., 2019; Nie et al., 2021), the environmental safety control effect cannot meet the construction requirements of water-rich soft soil. The freezing method, combined with steel sleeve receiving or starting shield technology in water-rich soft soil, can be an effective way to solve environmental safety control when receiving or starting shields in water-rich soft soil.

Many scholars have studied the end of tunnel construction and the connecting channel by using the freezing method. In terms of the measurement of the freezing temperature and displacement fields, Hu et al. (2019), Fan et al. (2019) and Fan et al. (2020) analyzed in detail the vertical frozen-soil

curtain at the end of the tunnel during freezing. The temperature distribution and surface deformation provide measured data for the freezing temperature field at the end of a large-diameter cross-river tunnel. For measured changes in deep soil frost heave and thawing and temperature development from freezing to complete thawing, Yang et al. (2017) showed that the freezing temperature change law is divided into five stages, and the thawing change law is divided into three stages. In addition, the vertical displacement change law of deep soil was obtained. The freezing method is reliable and safe, and it is widely used. However, because it is mostly used for shallow buried tunnels in urban rail transit, it is more sensitive to stratum changes caused by frost heave and thawing. Based on the effective prediction of frost heave and thawing deformation, Zheng et al. (2020) and Kang et al. (2021) used finite-difference numerical calculation to simulate the entire process of freezing method construction, and they comparatively studied the surface frost heaving, thawing deformation, and tube segment deformation caused by frozen-wall models with different thicknesses. The freeze wall thickness was optimized.

Scholars worldwide have carried out much research on the laws of formation frost heaving and thawing. Yan et al. (2013), Jiang et al. (2016) and Kang et al. (2020) controlled indoor water content, dry density, load conditions, and the number of freeze–thaw cycles through laboratory tests. The physical characteristics and temperature changes of silt after repeated frost heave and thawing were studied. Wang et al. (2017) and Li et al. (2015) experimentally studied the thawing characteristics of different soils at different freezing temperatures and analyzed the effects of the dry density and water content on the thawing of frozen soil. Wang et al. (2022a), Li et al. (2015) and Klas and Lars-Christer (2006) studied the effects of different parameters on the frost heave of frozen soil using laboratory model tests. To understand intuitively the laws of soil frost heaving, thawing, and deformation during the entire freezing process, the deformation differences of frozen walls of different thicknesses were compared to obtain prediction models that can effectively guide engineering applications and have greater practical significance. The numerical models show obvious superiority (Wang et al. (2020); Wang et al. (2021a)). Yuan et al. (2010) and others used the ADINA finite-element software to establish a numerical model of the freezing temperature field for the inflow section of a shallow buried tunnel, and they analyzed the effects of frozen-pipe spacing, salt water temperature, and frozen-pipe diameter on the frozen-wall development rate and frozen-wall thickness. The results show that artificial-freezing technology can effectively solve this special geotechnical engineering problem. Wu et al. (2006) analyzed and evaluated the deformation and stress of the frozen curtain of the Dalian Road tunnel freezing-method construction from the perspective of numerical methods. They found that the most unfavorable position of the curtain is at the point where the curtain contacts the existing tunnel. The analysis of the excavation process by Cheng et al. (2007) showed that quick freezing or intermittent freezing should be adopted in the freezing method to reduce the frost heave displacement caused by water migration. Some researchers, such as Hu X. et al. (2017), have verified the heat transfer of the cup-shaped frozen-soil curtain by numerical simulation. They found that the nature of the frozen soil and the crossing time of the frozen-soil curtain are related to the thermophysical properties of the soil in addition to the *in situ* soil moisture sensitivity.

Experimental research on the steel sleeve construction method has focused mainly on the characteristics analysis, construction control, and design improvement of the construction method. For example, Li and Lin (2009) summarized the design background and structural composition of the steel sleeve receiving auxiliary device. Zhao (2013) described a number of key technologies related to the steel sleeve receiving method. Xu (2014) optimized the design parameters of the steel sleeve structure and summarized the main points of the construction operation after optimization. Some of the forces and deformation laws of the steel sleeve during the shield-receiving period have also been analyzed. For example, Liao et al. (2016) used numerical simulation to analyze the field measurements of sleeve deformation and flood wall settlement and verified the feasibility of the steel sleeve receiving method.

Although there have been reports worldwide of typical freezing or steel sleeve method construction cases, the effect of the combined use of the two processes still lacks sufficient experimental data. Therefore, in this study, the shield construction of a typical soft soil layer in Suzhou, China, was studied. The applicability and safety of the freezing method combined with steel sleeve receiving-shield technology in water-rich soft soil were evaluated based on a field test system.

2 TEST AREA OVERVIEW

The research test area was selected from Tayuan Road to Zhuyuan Road Station of Subway Line 5 in Suzhou City, Jiangsu Province, eastern coastal area of mainland China. The earth pressure balance shield was used for the construction, and the total length of the shield section was approximately 929.47 m. A three-level underground structure with a ground elevation of +3.8 m, a shield tunnel center elevation of −17.750 m, channel centerline spacing of 10.55 m, shield center burial depth of approximately 21.3 m, hole diameter of 6.7 m, and segment thickness of 350 mm was used. The retaining structure is in the form of an underground continuous wall. The west end of Zhuyuan Road Station is located below Zhuyuan Road, an existing municipal road west of Binhe Road. Gas, water, sewage, rainwater, and other pipelines are stored in the surrounding area (**Figure 1**). According to the geological survey report, the soil layer distribution and physical and mechanical indices of the shield-receiving section are shown in **Figure 2**. Among them, the soil layers in the area reinforced by the tunnel are mainly 4_2 silty sand and silty soil and $(5)_1$ silty clay layer. The tunnel of the shield-receiving section is located in the sandy silt layer. This layer is a microaqueous aquifer. The risk of gushing water and sand easily occurs during construction. Moreover, the site conditions of the shield-receiving end are limited, and the groundwater level is high. The conventional method was used to reinforce the soil. Therefore, to receive the shield successfully, and in combination with the complicated engineering environment, it was decided to use a cup-shaped

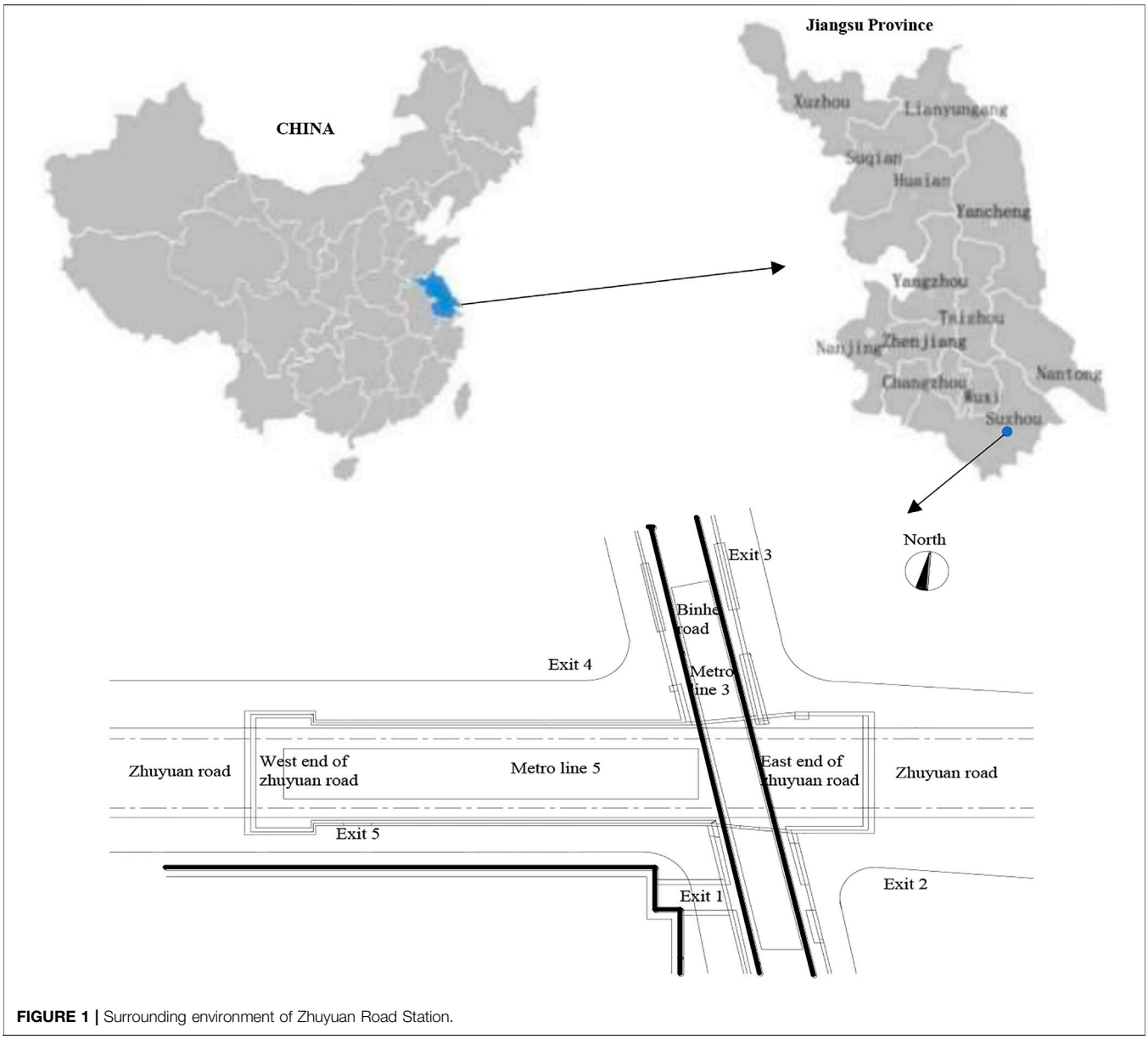

FIGURE 1 | Surrounding environment of Zhuyuan Road Station.

horizontal freezing method to strengthen the end and combine the steel sleeve to solve this problem (**Figure 3**).

3 TEST PLAN

3.1 Test Purposes and Construction Machinery Overview

3.1.1 Test Purposes

Based on the field test data, construction using the reinforced freezing method for the Suzhou water-rich soft soil layer, combined with a steel sleeve shield tunnel, was studied. The applicability and safety of the two combined receiving-shield technologies in water-rich soft soil were examined. The temperature change law of the frozen-soil curtain during the period of active freezing and maintenance freezing and the influence of the shield on the ground surface were analyzed when the freezing method was combined with the steel sleeve.

3.1.2 Construction Machinery Overview

3.1.2.1 Shield and Freezing-Station Layouts

The shield receiving in the Tazhu section is set at the Zhuyuan Road Station, and one Liaoning Sansan shield machine is used for construction. The main components of the shield machine include the front shield, middle shield, tail shield, segment installation machine, and screw conveyor. The cutter head, rear trailer, and accessories.

The freezing station is set close to the vent of the station, covering an area of approximately 100 m^2. The equipment in the station mainly includes the freezer, brine tank, brine pump, clean

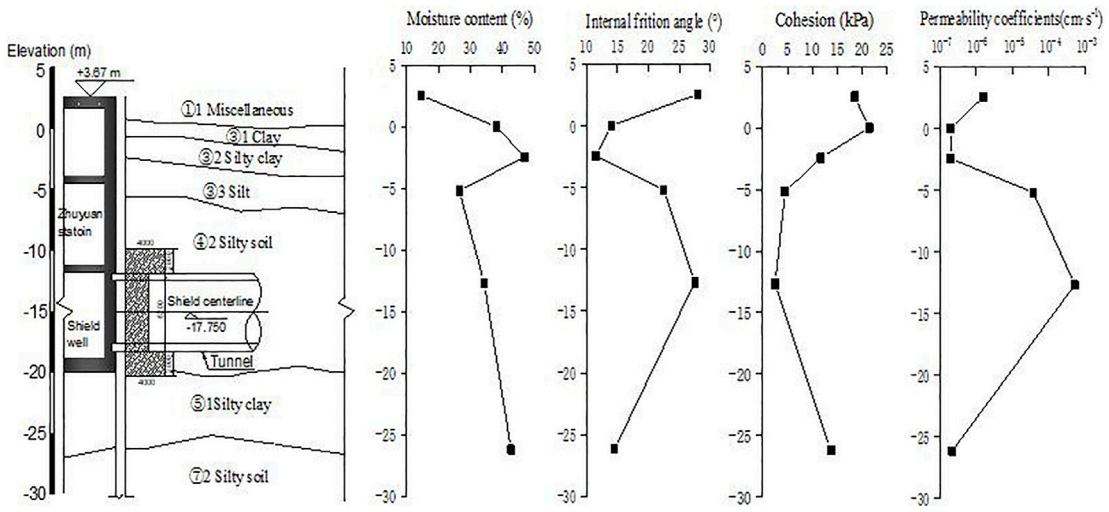

FIGURE 2 | Soil distribution in shield well area.

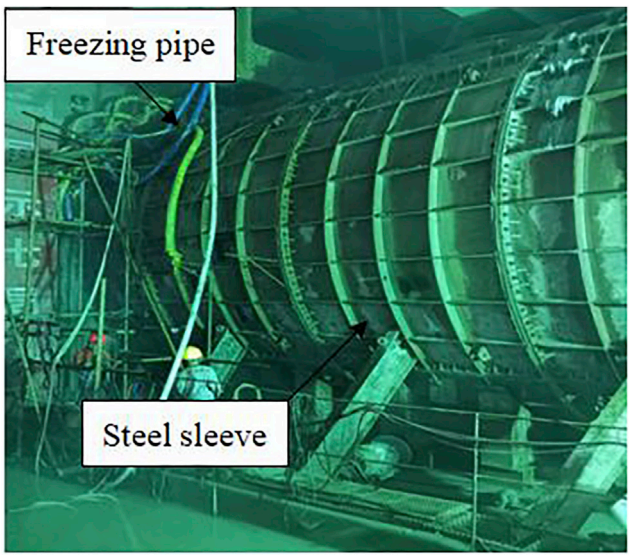

FIGURE 3 | In site freeze pipes at the shield machine launching shaft.

water pump, and cooling tower. For cooling-water circulation, two KYLR150-315A-type clean-water pumps are used, one for each standby. The freezing pipelines are laid with water distributors from the top of the cave door, without affecting the shield turning head and installing the steel sleeve in the receiving well.

3.1.2.2 Steel Sleeve Receiving

The steel sleeve receiving method is based on the design concept of the balanced arrival of the shield. Injecting a filler (clay soil, water, etc.) with a certain pressure and fluidity into the steel sleeve pushes the shield through the steel sleeve. The pressure in the cabin is always in equilibrium.

Steel sleeve shield reception is a safe and effective method. It can ensure that, when the surrounding environment is complex or in the water-rich sand layer, the tunnel door seal does not leak when the shield is received. In the case of weak water-rich formations or complex geological conditions, it is not sufficient to rely on the rubber door curtain and the door pressure plate to seal the door. The shield has a risk of water and sand coming through the door. Therefore, a steel sleeve is installed in the receiving well and connected to the door; thus, when the shield machine penetrates into the sealed environment inside the steel sleeve, the risk of water and sand leakage when the shield machine is out of the hole can be avoided.

3.1.2.3 Steel Sleeve Structure Design

The steel sleeve receiving system is composed of a barrel structure, bottom frame, I-beam support, back shield system, rear-end cover, feed port, and slurry injection and discharge pipe. As shown in **Figure 4**, the barrel material is made of a 20-mm-thick steel plate, and the outer circumference of each section of the barrel is welded with longitudinal and circumferential plate ribs to ensure the rigidity of the barrel. The thickness of the rib is 20 mm, the height is 120 mm, and the interval is approximately 550–600 mm. The ends of each section of the cylinder and the upper and lower semicircular joint surfaces are welded with a round flange. The flange uses a 40-mm-thick plate. M30 and 8.8 bolts are used between the four cylinders and between the two cylinders, and a 10-mm-thick rubber pad was added in the middle to ensure the sealing effect of the steel sleeve.

3.2 Test Implementation Plan and Design Parameters

The main construction process of this test includes the freezing method, steel sleeve installation, and shield receiving. In the freezing method construction process, the freezing-station

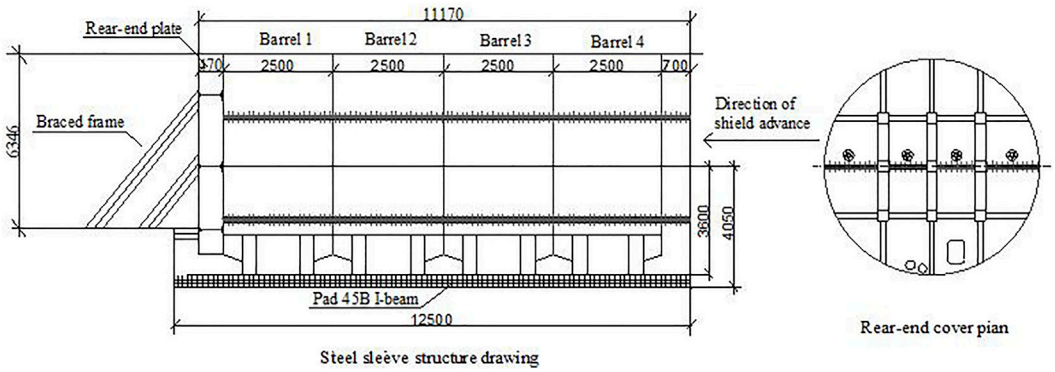

FIGURE 4 | Structural drawings of steel sleeve.

TABLE 1 | Frozen-curtain parameters.

Project	Parameter	Project	Parameter
Freezing tube	Φ89 × 10 mm, 20 # low carbon steel seamless steel pipe	Active freeze time	35 days
Temperature tube	Φ89 × 10 mm, 20 # low carbon steel seamless steel pipe	Brine temperature	−28°C ~ −30°C
Number of frozen holes	Frozen holes 57, 5 temperature measuring holes	Frozen-wall uniaxial compression	4.0 MPa
Total length of freezing tube	309.8 m	Flexural strength	2.0 MPa
Freeze curtain thickness	2 m	Shear strength	1.8 MPa
Average frozen-wall temperature	−10°C ~ −15°C	Total cooling requirement	3.2×10^4 Kcal/h

installation and drilling construction are carried out at the same time. After the drilling construction is completed, the freezer installation and freezing phases are transferred. Through the observation and calculation of each measuring point in the temperature measurement hole, it is determined that the frozen soil and the ground connection wall are completely cemented, and the frozen-soil curtain intersects. When the design strength is reached, the shield starts to advance. The process stops immediately, the ground connecting wall is removed to 0.85 m, the frozen pipe in the opening of the tunnel is removed, and, finally, shield tunneling is implemented. The design parameters are listed in **Table 1**.

The construction procedure of the steel sleeve is as follows.

The connection of the main part → the connection of the transitional connection plate of the steel sleeve and the steel ring of the door → support installation → tightness inspection → mortar base installation. Before the steel sleeve installation, first determine the center line of the line in the foundation pit—that is, the centerline of the steel sleeve—when the steel sleeve is positioned, the two control lines of the bottom line of the steel sleeve and the centerline of the line must coincide. After the steel sleeve is assembled as a whole, it is lifted up to make the steel sleeve. The center of the line coincides with the centerline of the predetermined line, moves toward the door as a whole, leans against the door, and is welded to the steel ring of the door. After the steel sleeve is installed, the cylinder position is retested, inspected, and shielded. It is determined whether the centerlines reached by the airshaft coincide.

Shield-Receiving Construction Process

The use of a steel sleeve to receive the shield construction includes a series of key procedures, such as the removal of the door, the installation and positioning of the steel sleeve, and the tightness test. The shield machine is pushed into the steel sleeve, and the shield is grouted. The door is sealed, the shield machine is received, the steel sleeve is removed, etc. Before the shield arrives, the height difference between the center of the hole at the west end and the floor is 4,050 mm, and the height difference between the center of the door and the bottom of the steel sleeve is 3,600 mm. Therefore, the bottom of the bracket has a 45-mm I-steel pad height of 450 mm, to ensure the smooth performance of the shield advance. During the advancement of the shield, the shield must pass through the reinforced area, pass the door structure of the station, and then reach the steel sleeve. In this process, the advance speed and total thrust should be strictly controlled, the shield construction parameters and attitude should be controlled, and the steel sleeve should be monitored in real time. Force and deformation data of the cylinder are used to adjust the shield parameters over time.

The advancement construction of the shield-receiving section is divided into three stages. The shield advances to the cutter head to add solids at a distance of 1 m and enters the frozen and solidified tunneling stage of the steel sleeve. According to engineering experience, the speed of the shield in the first stage should be controlled at 10–20 min and a thrust T1 < 15,000 kN. The speed of the second stage should be controlled at 5–10 mm/min and a thrust T2 < 8,000 kN. The speed of the

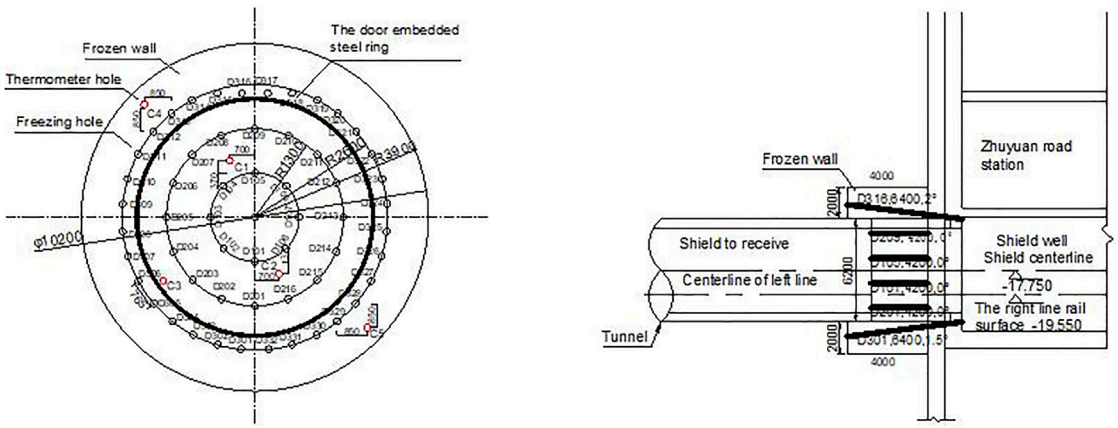

FIGURE 5 | Frozen hole and temperature hole layout (unit: mm): **(A)** elevation view and **(B)** sectional view.

third stage should be controlled at <5 mm/min and a thrust T3 < 4,000 kN.

3.3 Freezing Hole and Temperature Measuring Hole Arrangement

3.3.1 Freezing Hole Layout

The freezing method, as a method of soil consolidation with a strong water-sealing effect and almost no impact on the environment, is widely used in water-rich soft soil layers. According to the geological conditions and construction conditions, this project adopts the construction scheme of horizontal freezing and strengthening of boreholes in working wells. The specific arrangement of the frozen holes and temperature-measuring holes is shown in **Figure 5**. According to the design of the frozen curtain, the frozen holes of the receiving door are horizontally angled. Fifty-seven frozen holes are arranged. Among them, the cup wall freezing holes are arranged circularly along an opening of φ7.8 m, the opening spacing is 0.765 m (chord length), the number of frozen holes is 32, and the length is 6.4 m. The freezing holes at the bottom of the cup are arranged circularly along openings of φ5.2 and φ2.6 m. The intervals of the openings are 1.019–0.998 m (chord length), the number of frozen holes is 24, the length is 4.2 m, the center of the opening is one frozen hole, and the length of the frozen hole is 2 m. The terminal was actively frozen for 35 days. Before acceptance, an acceptance inspection should be performed to determine the thickness of the frozen wall through the temperature measurement hole and to ensure that the average temperature meets the design requirements—the average design temperature of the frozen wall of the frozen body cup wall is less than −10°C. (The average design temperature of the frozen wall at the bottom of the cup is less than −15°C.) The frozen wall and the continuous wall are completely glued, and the average temperature at the measurement point at the junction is less than −5°C.

3.3.2 Temperature Hole Arrangement

To measure the temperature development status of different positions of the freezing curtain range and understand the development law of the freezing temperature field, five temperature measuring holes were arranged in the receiving cave door with a depth of 3.9–6.4 m. The aim was to adopt corresponding control measures comprehensively to ensure the safety of construction. In each temperature measuring hole, one to seven measuring points were set. A measuring point was set at every 1-m interval, with a large distance between the final holes. The positions of the temperature measuring holes (C1–C5), where each point is evenly distributed along the hole depth—specifically, holes C1–C3 with a depth of 3.9 m, each with a temperature measurement point at depths of 1, 2, 3, and 3.9 m, and holes C4–C5 with a depth of 6.4 m, a temperature measuring point was arranged for every at depths of 1, 2, 3, 4, 5, 6, and 6.4 m. The temperature measurement point number of each hole is Ci-j (i indicates the number of temperature measurement holes, and j indicates the number of measurement points), as shown in **Figure 6**.

3.4 Arrangement of Ground Settlement Points

The shield construction process has a large impact on the ground deformation. To control the ground settlement strictly, the monitoring points were laid out along the tunnel axis according to the section. Within 100 m of the shield-receiving section, a section was set every 5 m, and a single line was arranged for each monitoring section. There were two settlement observation points, and a cross section was set every 10 m in the remaining sections. The horizontal distance between the observation points was 2.5–5 m. The specific arrangement is shown in **Figure 7**.

3.5 Steel Sleeve Measurement and Monitoring

When the shield reached the steel sleeve, the measurement frequency was increased, and the control points were reviewed to ensure that the shield reaches the correct posture. A

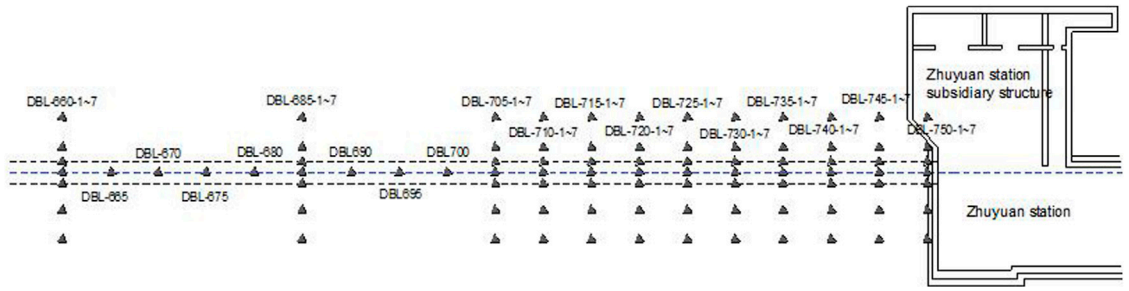

FIGURE 6 | Site layout of the west end of Zhuyuan Road Station.

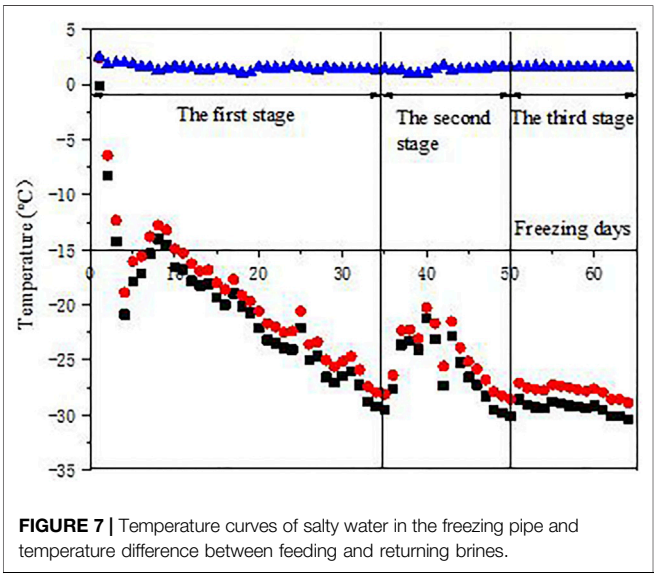

FIGURE 7 | Temperature curves of salty water in the freezing pipe and temperature difference between feeding and returning brines.

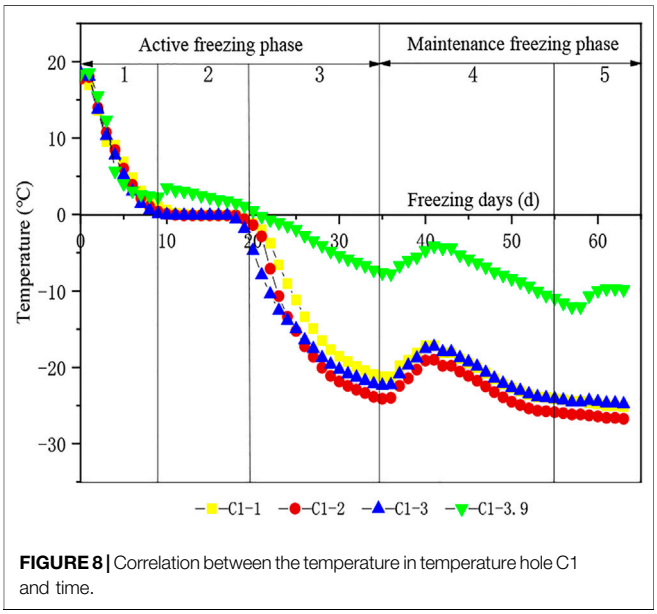

FIGURE 8 | Correlation between the temperature in temperature hole C1 and time.

monitoring point was arranged before the shield machine arrived to monitor the shield entry sleeve displacement. According to the analysis of the steel sleeve displacement monitoring data, if the deformation is large, it is necessary to take targeted measures.

4 FREEZE MONITORING AND DATA ANALYSIS

4.1 Measured Analysis of Deloop Brine

After the project starts to freeze, the monitoring results of the temperature measurement point of the main circuit of the brine loop are shown in **Figure 7**.

The data show that the temperature change of the brine return circuit can be roughly divided into three stages. In the first stage, during the rapid decline of the brine temperature, which lasted approximately 6 days, the temperature dropped from 2.5°C to −21°C, and the average cooling rate was 3.92°C/d. The temperature difference of the return circuit was large. The temperature difference of the return circuit reached 2.5°C at the beginning of freezing. With the passage of time, the temperature difference of the return circuit gradually decreased. In the second stage, the slowdown stage lasted approximately 28 days, the temperature dropped from −21°C to −28°C, and the average cooling rate was 0.25°C/d. In the third stage, the temperature of the brine increased slightly because of the rupture of the freezing tube, which caused the freezing time to extend. This stage lasted about 16 days, and the temperature returned to approximately −28°C. Then, the temperature of the brine was maintained at approximately −28°C to −29°C. The temperature of the brine route reached −29.0°C, the circuit reached −28.2°C, and the temperature difference between the brine and the circuit was less than 2.0°C.

4.2 Measured Analysis of Soil Temperature

Before the shield machine is started, the thickness of the frozen curtain must meet the design requirements of 2 m. The temperature of the frozen soil around the shield must not be lower than −5°C and close to zero, which can ensure that the water is solid. At 2°C, all the design requirements must be met before the door can be broken. **Figures 8–12** show the monitoring

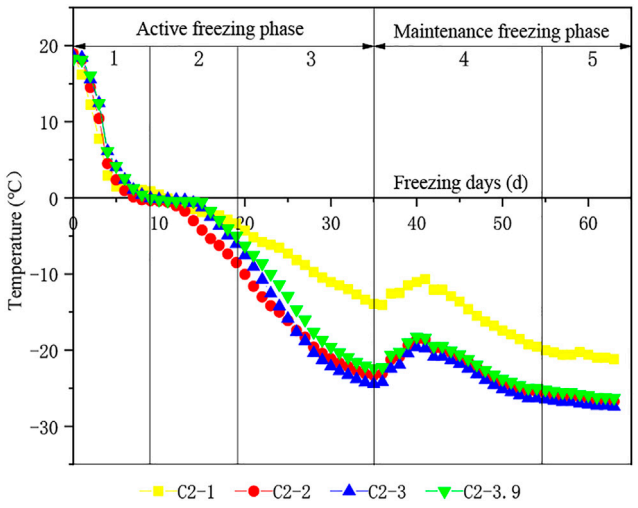

FIGURE 9 | Correlation between the temperature in temperature hole C2 and time.

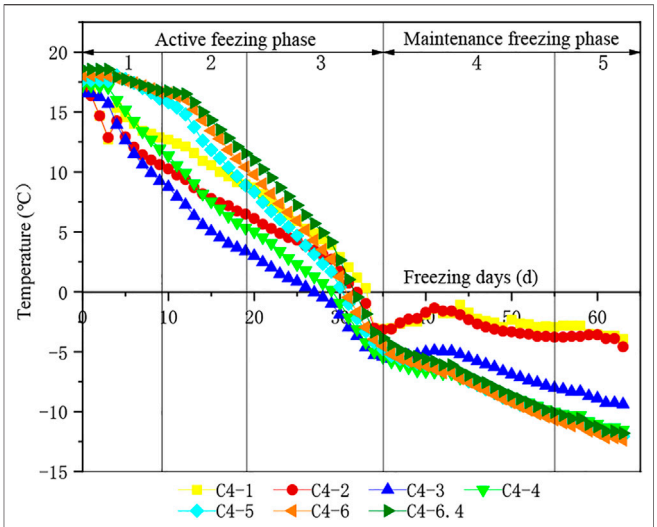

FIGURE 11 | Correlation between the temperature in temperature hole C4 and time.

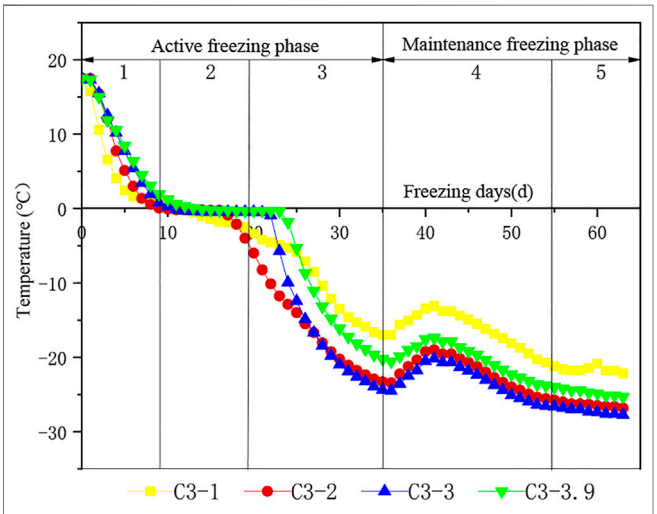

FIGURE 10 | Correlation between the temperature in temperature hole C3 and time.

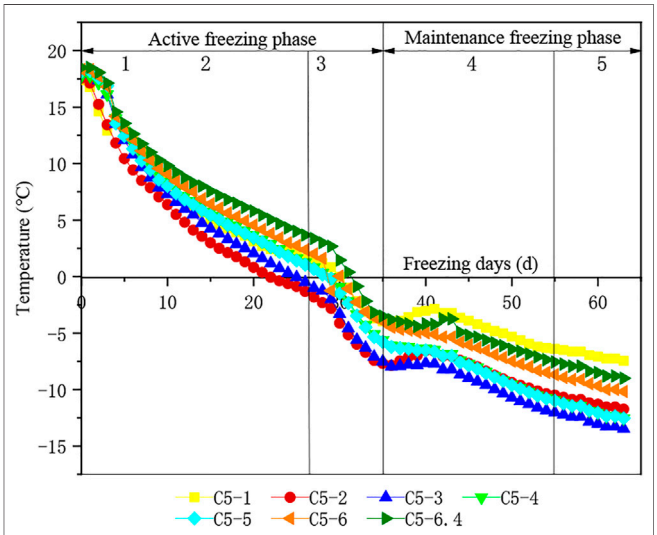

FIGURE 12 | Correlation between the temperature in temperature hole C5 and time.

data of the temperature at each temperature measuring point during the freezing period for the freezing, excavation, and maintenance freezing of the cave door.

4.2.1 Change Law of Soil Temperature Over Time

During freezing, the temperature changes of the measuring points in the temperature measuring hole were roughly the same, and they can be divided into five stages. The temperature measuring holes C1, C2, and C3 were located inside the frozen wall, and the temperature measuring holes C4 and C5 were located in the outer ring of the frozen wall. **Figures 8–12** show that the temperature changes of the temperature measuring holes C1, C2, and C3 were similar, and the temperature changes of the temperature measuring holes C4 and C5 were similar. The inward development speed of the frozen wall was much higher than the outward development speed. For temperature measuring holes C1, C2, and C3, the first stage was as follows. At the beginning of the active freezing stage, the formation temperature was high, and the temperature difference between the salt water and the formation was large. Therefore, the temperature of the soil body decreased rapidly, and the temperature of the temperature measuring hole changed rapidly. As the temperature decreased, the temperature difference between saline water and soil became increasingly smaller, and the temperature change rate gradually decreased. This stage lasted approximately 8 days, and the average cooling rate reached 2.13°C/d. The second stage was the middle of the active

freezing stage. The temperature of the warm hole was close to 0°C. Owing to the influence of the latent heat of the water, the temperature of the soil decreased slowly, and the temperature of the temperature measuring point changed slowly. This stage lasted approximately 10 days, and the average rate reached 0.15°C/d. The freezing curtain around the freezing tube gradually intersected to form a frozen wall, the speed became faster, and the thickness of the frozen wall increased faster. In the third stage, in the late stage of the active freezing phase, the soil temperature was less than 0°C, and the water formed ice to produce latent heat. At that time, the soil temperature began to drop rapidly, and the temperature at the measuring point of the temperature measuring hole dropped rapidly. This stage lasted approximately 17 days, and the average rate reached 1.47°C/d. For the C4 and C5 temperature measuring holes, the temperature changes were similar, because it is far away from the freezing wall, the temperature is close to 0°C on the 26th and 28th days, respectively, and the phase transition is reached. The rates were 0.69°C/d and 0.64°C/d, respectively. At the end of the active freezing phase, the latent heat of water formation was completed, at which time the soil temperature began to drop rapidly, and the temperature reached −5°C and −8°C, respectively, at the end of the active freezing phase. The fourth stage is the initial stage of the maintenance freezing phase because of temperature inertia. The freezing wall was still slowly expanding, during which the amount of frost heaving reached the maximum. However, the temperature of the brine increased slightly because of the rupture of the frozen pipe caused by construction, and the freezing time was extended. This stage lasted approximately 20 days, and the temperature reached approximately −25°C. The fifth stage was maintenance at the end of the freezing phase. The temperature at this stage remained basically unchanged and was maintained at −28°C to −29°C. The difference in circuit temperature was less than 2°C, which was in line with the design value.

The picture shows that the temperature gradient of the measurement point with a smaller penetration depth was smaller than the measurement point with a larger penetration depth. In the initial freezing stage, the temperature of the measurement point with a small penetration depth was lower than that of the measurement point with a large penetration depth. When the freezing curtain formed, the temperature of the measuring point with a smaller penetration depth was slightly higher than the temperature of the measuring point with a larger penetration depth. This is because the convective heat dissipation of the surface of the segment affected the temperature drop of the soil near the segment, so the temperature changed more slowly at the measuring point near the segment. The temperature measuring holes C1, C2, and C3 were located inside the frozen wall, closer to the excavation surface, and were more affected by the excavation. The temperature measuring holes C4 and C5 were located outside the frozen wall, far away from the excavation surface, and are less affected by the excavation, except that the temperature at the measuring points (C4-1 and C4-2) at the segment increased. The remaining measuring points remained unchanged.

4.2.2 Development Rate and Temperature Distribution of Frozen Wall

The times for the temperature of the temperature measuring holes C1, C2, C3, C4, and C5 to reach 0°C were 10, 9, 9, 26, and 28 days, respectively—that is, the rates of reaching 0°C were 1.8°C/d, 2.11°C/d, 2°C/d, 0.69°C/d, and 0.64°C/d, respectively. From this, it can be calculated that, when the frozen wall reaches C1, C2, C3, C4, and C5, the development speeds of the frozen wall are 39.8, 38.7, 30.5, 22.8, and 21.3 mm/day. Therefore, it can be concluded that the freezing wall develops inward more quickly. This requires more study, because the soil on the inside of the frozen wall that participates in heat conduction is less than that outside, and it is affected by the heat absorption of the low-temperature brine in the frozen tube at the top. Thus, development is faster (Han et al., 2015; Liao et al., 2016).

4.3 Freezing Effect Analysis

According to the temperature measurement, the C5 temperature measurement hole was an outer-ring temperature measurement hole, with a depth of 6.4 m (4.4 m deep in the soil). The 6.4-m measurement point was the most unfavorable temperature measurement point. The temperature measurement value was −2.1°C. For the T5 temperature measurement, the temperature of the 6.4-m hole was used to check the frozen-wall thickness and average frozen-wall temperature. The calculation is as follows.

4.3.1 Calculation Formula for the Frozen-Cylinder Radius

$$r_2 = \exp\left(\frac{t_1 lnr - lnr_1}{t_1 - t}\right) = 1.45 \quad (1)$$

In the formula:

Circuit brine temperature $t_1 = -28.7$°C.

Distance between the temperature measuring hole and freezing tube r = 1.1 m.

Radius inside freezing tube $r_1 = 0.0345$ mm.

Measuring hole temperature t = −2.1°C.

Calculated frozen-cylinder radius $r_2 = 1.45$ m

$$E = 2\sqrt{r^2 - \left(\frac{l}{2}\right)^2} = 2.75 \quad (2)$$

In the formula:

Maximum distance of the frozen tube l = 0.9 m.

Freezing cylinder radius r = 1.45 m.

The calculated thickness of the most unfavorable position of the frozen wall E = 2.75 m, which meets the requirements of a design greater than 2 m.

4.3.2 Average Temperature of Frozen Wall

According to the soil temperature measured at the site, the average temperature of the frozen wall of the section was calculated using the ice-forming formula.

FIGURE 13 | Measured hole survey.

$$t = t_b\left(1.135 - 0.325\sqrt{l} - 0.875\frac{1}{\sqrt[3]{E}} + 0.266\frac{\sqrt{L}}{E}\right) - 0.466 + 0.25t_B = -10.42℃ \quad (3)$$

In the formula:

t = average temperature of effective thickness of frozen wall, ˚C

t_b = brine temperature, −28.7˚C

l = freezing hole spacing, 0.9 m.

E = frozen-wall thickness, 2.75 m

t_B = wellside frozen-soil temperature, −2.1˚C.

According to the ice-forming formula, the average temperature of the frozen wall is t = −10.42˚C, which is lower than the design requirement of −10˚C.

To verify further the reinforcement quality of the tip well and ensure the safe reception of the shield machine, horizontal drilling was carried out from September 15 to 16 September 2019, and nine drilling holes with a depth of 2 m were drilled. The arrangement of the exploration holes is shown in **Figure 13**. During the construction of the exploration holes in the frozen wall, according to the site observations, the soil was dense and free of water leakage and sand leakage.

Based on the above comprehensive analysis, according to the freezing temperature, the development trend of the temperature measuring hole, and the thickness of the frozen wall, it can be determined that the wall breaking condition has been reached.

4.4 Measured Analysis of Surface Subsidence

Many factors affect ground subsidence, including the construction of frozen holes, the removal of tunnel doors, and the tunneling of shields (Mei et al., 2016; Mei et al., 2019; Lai et al., 2020; ; Wang et al., 2022b). In this study, the effects of shield tunneling on ground surface changes were mainly examined. The specific layout of the surface monitoring points is shown in **Figure 6**. The measurement point DBL-i-4 (where i is the measurement point numbers 705–745) was selected for analysis of the shield centerline. The measurement point of DBL-750-4 was destroyed, and no measurement data were available. The measured results are shown in **Figure 14**. Because of the influence of the construction conditions, surface subsidence monitoring near the western end was started 20 days after the freezing hole was constructed. The freezing hole was actively frozen for 35 days, and the maintenance freeze was 20–25 days—that is, the active freezing ends at 15 days in the picture. After the freezing started, the ground deformation was small, because the soil was not frozen in the early stage. At that time, the ground settlement caused by the shield was greater (Li Z. et al., 2021; Sheng et al., 2021; Wang et al., 2021b; Wang J. et al., 2022) and the farther away from the frozen end, the greater the settlement. After 30 days of freezing, the frozen-curtain crossing circle was basically completed. Then, the surface settlement near the frozen body began to decrease, and, the closer to the frozen body, the smaller the influence of the shield on the ground deformation. The initial period of maintenance freezing lasted approximately 15 days. Owing to the temperature inertia, the frozen wall continued to expand slowly, and the amount of frost heave during this period reached its maximum. The freezing method, combined with the steel sleeve effect, was sufficient to resist the impact of the shield on the ground surface, and the surface settlement appeared positive. The effect was more obvious as it got closer to the frozen surface, such as the measurement points DBL-725–745. During the later period of the maintenance freeze until the receiving period of the shield, the shield gradually approached the frozen body, and its influence on soil deformation increased continuously. The surface settlement value began to increase and changed from positive to negative.

5 DISCUSSION

In the construction scheme, in which the horizontal freezing method was combined with a steel sleeve, freezing technology froze the surrounding soil, so that the soil could remain stable when the ground wall was broken, reducing the risk of poor soil self-reliance when the tunnel door was broken. The enclosed space of the steel sleeve provided balanced water and earth pressure on the palm face, which greatly reduced the risk of water and sand gushing through when the shield was received. The key to the combined application of the two receiving measures was determining whether the equilibrium pressure between the steel sleeve and the cavity of the negative ring segment could be balanced with the actual water and earth pressure in time after the door was broken. Owing to the large range of soil freezing and strengthening, cutter head freezing accidents are likely to occur when the shield passes through the frozen-soil wall. Therefore, it is necessary to ensure that the shield is normal, does not stay, and passes quickly to prevent the shield from being frozen. Therefore, preventing the shield cutter head from freezing was also one of the key points to be controlled in this project. In addition, the shield-receiving construction scheme combined with the freezing method and the steel sleeve has a small floor area, convenient construction, a small impact on the surrounding environment, good safety, and good construction prospects.

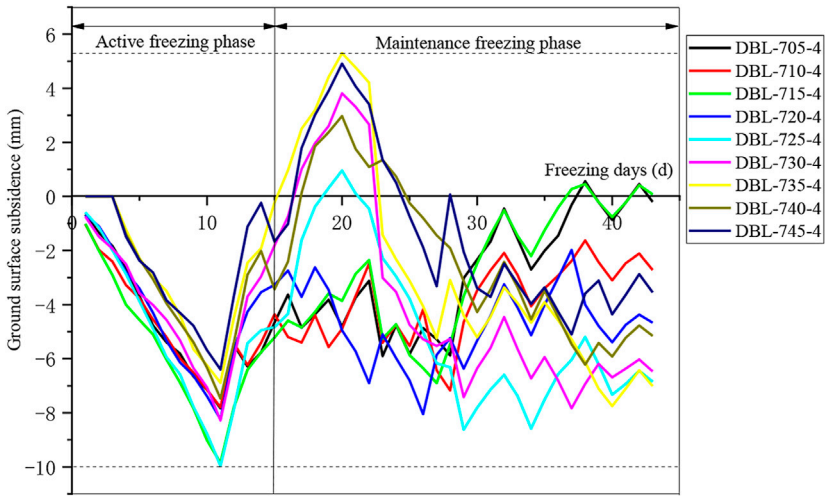

FIGURE 14 | Cumulative value of ground surface freezing and steel sleeve receiving at the western end of Zhuyuan Road.

6 CONCLUSION

1) The freezing method, combined with steel sleeve receiving-shield technology, in water-rich soft soil can not only reduce the risk of poor self-reliance of the soil when the door is broken, but also greatly reduces the gushing water when receiving the shield. The risk of sand gushing is reduced, the craft covers a small area, and the construction is convenient. These characteristics can effectively reduce the environmental disturbance caused by shield construction and have good promotion and application value.
2) During the freezing period of water-rich soft soil, the temperature change trends of the measuring points in the temperature measurement hole are roughly the same. The freezing process can be divided into a rapid cooling period, slow cooling period, medium rapid cooling period, stable soil temperature period, and maintenance freezing period. In the five typical stages, special attention is paid to the changes in the soil settlement when the various stages are changed during construction to prevent sudden changes in soil displacement.
3) When the water-rich soft soil is frozen, the closer the active freezing period is to the inside of the frozen-soil curtain, the faster the development rate of the frozen wall. At the same time, the temperature gradient of the soil body increases with increasing radial depth. After the curtain circle has been frozen, the frost heaving of the soil accelerates significantly until the amount of frost heave peaks. The influence of shield tunneling on ground settlement is large, but the combination of the freezing method and steel sleeve can somewhat suppress this effect.

DATA AVAILABILITY STATEMENT

The original contributions presented in the study are included in the article/Supplementary Material, further inquiries can be directed to the corresponding author.

AUTHOR CONTRIBUTIONS

YM, CL and J-TZ conceived and designed the methods, provided the guide of monitoring and theoretical research for the study,and economically supported the project. YM, Y-YL and XY completed the data analysis and the writing of paper manuscript.

FUNDING

This research was supported by the National Natural Science Foundation of China (52178302) and the Key R&D Program of Shaanxi Province (2020SF-373).

REFERENCES

Cheng, H., Yao, Z. S., Zhang, J. S., and Rong, C. X. (2007). Experimental Study on Frost Heaving and Thawing Settlement of Tunnels Constructed by Artificial Horizontal Freezing Method. *J. Civil Eng.* (10), 80–85. doi:10.15951/j.tmgcxb.2007.10.004

Ding, Z., Hong, Q. H., Wei, X. J., Zhang, M. Y., and Zheng, Y. (2017). Microscopic Experimental Study on Artificially Frozen and Thawed Soft Soil under Subway Train Loads. *J. Zhejiang Univ. (Engineering Edition)* 51 (07), 1291–1299. doi:10.3785/j.issn.1008-973X.2017.07.004

Dong, Z., Kuo, C., Yin, J., Wen, S., Liu, G., and Gou, Y. (2021). Examination of Longitudinal Seismic Vulnerability of Shield Tunnels Utilizing Incremental Dynamic Analysis. *Front. Earth Sci.* 9, 995. doi:10.3389/feart.2021.779879

Fan, J., Jiang, D., Liu, W., Wu, F., Chen, J., and Daemen, J. (2019). Discontinuous Fatigue of Salt Rock with Low-Stress Intervals. *Int. J. Rock Mech. Mining Sci.* 115 (3), 77–86. doi:10.1016/j.ijrmms.2019.01.013

Fan, J., Liu, W., Jiang, D., Chen, J., Tiedeu, W. N., and Daemen, J. J. K. (2020). Time Interval Effect in Triaxial Discontinuous Cyclic Compression Tests and Simulations for the Residual Stress in Rock Salt. *Rock Mech. Rock Eng.* 53 (9), 4061–4076. doi:10.1007/s00603-020-02150-y

Han, L., Ye, G.-L., Li, Y.-H., Xia, X.-H., and Wang, J.-H. (2015). *In Situ* monitoring of Frost Heave Pressure during Cross Passage Construction Using Ground-Freezing Method. *Can. Geotech. J.* 53 (3), 530–539. doi:10.1139/cgj-2014-0486

Hu, J., Liu, W., Pan, Y., and Zeng, H. (2019). Site Measurement and Study of Vertical Freezing Wall Temperatures of a Large-Diameter Shield Tunnel. *Adv. Civil Eng.* 2019, 1–11. doi:10.1155/2019/8231458

Hu, J., Liu, Y., Wei, H., Yao, K., and Wang, W. (2017). Finite-Element Analysis of Heat Transfer of Horizontal Ground-Freezing Method in Shield-Driven Tunneling. *Int. J. Geomech.* 17 (10), 04017080. doi:10.1061/(asce)gm.1943-5622.0000978

Hu, X. D., Fang, T., Guo, X. D., and Ren, H. (2017). Field Measurement of Defrosting Temperature Field of Gongbei Tunnel Tube Curtain Freezing Field Test. *J. China Coal Soc.* 42 (07), 1700–1705. doi:10.13225/j.cnki.jccs.2016.1246

Jiang, D., Fan, J., Chen, J., Li, L., and Cui, Y. (2016). A Mechanism of Fatigue in Salt under Discontinuous Cycle Loading. *Int. J. Rock Mech. Mining Sci.* 86 (7), 255–260. doi:10.1016/j.ijrmms.2016.05.004

Kang, Y., Fan, J., Jiang, D., and Li, Z. (2020). Influence of Geological and Environmental Factors on the Reconsolidation Behavior of fine Granular Salt. *Nat. Resour. Res.* 30 (1), 805–826. doi:10.1007/s11053-020-09732-1

Kang, Y., Geng, Z., Lu, L., Chen, L., Liu, X., Liu, B., et al. (2021). Compound Karst Cave Treatment and Waterproofing Strategy for EPB Shield Tunnelling in Karst Areas: A Case Study. *Front. Earth Sci.* 9, 848. doi:10.3389/feart.2021.761573

Klas, H., and Lars-Christer, L. (2006). Water Content Reflectometer Application to Construction Materials and its Relation to Time Domain Reflectometry. *Cold Regions Sci. Technol.* 44 (1), 20–37. doi:10.2136/vzj2005.0053

Lai, J., Zhou, H., Wang, K., Qiu, J., Wang, L., Wang, J., et al. (2020). Shield-Driven Induced Ground Surface and Ming Dynasty City wall Settlement of Xi'an Metro. *Tunnelling Underground Space Technol.* 97, 103220. doi:10.1016/j.tust.2019.103220

Li, F., and Lin, B. (2009). Design of Assistance Device for Shield Arrival and Reception. *Building mechanization* 30 (09), 66–68. doi:10.13311/j.cnki.conmec.2009.09.008

Li, G. Y., Sun, Z. L., Li, S., Huang, S., and Xu, Q. W. (2019). Research on Construction Technology of Shield Steel Sleeve Receiving in Sandy Cobble Stratum. *Transportation Res.* 5 (03), 72–78. doi:10.16503/j.cnki.2095-9931.2019.03.010

Li, X., Yang, S., Wang, Y., Nie, W., and Liu, Z. (2021). Macro-micro Response Characteristics of Surrounding Rock and Overlying Strata towards the Transition from Open-Pit to Underground Mining. *Geofluids* 2021, 1–18. doi:10.1155/2021/5582218

Li, Y., Li, D. W., and Chen, J. H. (2015). Experimental Study on Frost Heave Characteristics of Artificial Frozen clay. *Coal Eng.* 47 (02), 126–129. doi:10.11799/ce201502041

Li, Z., Chen, K., Li, Z., Huang, W., and Wang, X. (2021). Deterioration and Cavity of Surrounding Rocks at the Bottom of Tunnel under the Combined Action of Heavy-Haul Load and Groundwater: An Experimental Study. *Front. Earth Sci.* 9, 1177. doi:10.3389/feart.2021.779578

Liao, S. M., Men, Y. Q., and Zhao, G. Q. (2016). Mechanical Behaviors and Field Tests of Steel Sleeves during Shield Receiving. *Chin. J. Geotechnical Eng.* 38 (11), 1948–1956. doi:10.11779/CJGE201611003

Mei, Y., Hu, C.-M., Yuan, Y.-L., Wang, X.-Y., and Zhao, N. (2016). Experimental Study on Deformation and Strength Property of Compacted Loess. *Geomech. Eng.* 11 (1), 161–175. doi:10.12989/gae.2016.11.1.161

Mei, Y., Li, Y.-L., Wang, X.-Y., Wang, J., and Hu, C.-M. (2019). Statistical Analysis of Deformation Laws of Deep Foundation Pits in Collapsible Loess. *Arab J. Sci. Eng.* 44 (10), 8347–8360. doi:10.1007/s13369-019-03931-6

Nie, Q. K., Sun, G., Gao, S. Y., and Liu, H. T. (2021). Disturbance Process of sandy Gravel Stratum Caused by Shield Tunneling and Ground Settlement Analysis. *Front. Earth Sci.* 9, 994. doi:10.3389/feart.2021.782927

Ren, H., Hu, X. D., Hong, Z. Q., and Zhang, J. (2019). Experimental Study on the Active Freezing Scheme of the Pipe Curtain Freezing Method for Ultra-shallow Buried Tunnels. *Chin. J. Geotechnical Eng.* 41 (02), 320–328. doi:10.11779/CJGE201902010

Sheng, G., Wen, S., Wu, F., Liu, S., and Wang, Z. (2021). Effects on a Nearby Bridge of Dismantling Temporary Lining during Excavation of a Shallow-Buried Rectangular Tunnel. *Front. Earth Sci.* 9, 802662. doi:10.3389/feart.2021.802662

Wang, J., Wang, T., Song, Z., Zhang, Y., and Zhang, Q. (2021a). Improved Maxwell Model Describing the Whole Creep Process of Salt Rock and its Programming. *Int. J. Appl. Mech.* 13, 21501131. doi:10.1142/S1758825121501131

Wang, J., Wang, X., Zhang, Q., Song, Z., and Zhang, Y. (2021b). Dynamic Prediction Model for Surface Settlement of Horizontal Salt Rock Energy Storage. *Energy* 235, 121421. doi:10.1016/j.energy.2021.121421

Wang, J., ZhangSong, Q. Z. P., Song, Z., Feng, S., and Zhang, Y. (2022). Nonlinear Creep Model of Salt Rock Used for Displacement Prediction of Salt Cavern Gas Storage. *J. Energ. Storage* 48, 103951. doi:10.1016/j.est.2021.103951

Wang, J., ZhangSong, Q. Z. P., Song, Z., and Zhang, Y. (2020). Creep Properties and Damage Constitutive Model of Salt Rock under Uniaxial Compression. *Int. J. Damage Mech.* 29 (6), 902–922. doi:10.1177/1056789519891768

Wang, X. B., Hu, J., and Ju, J. (2017). Three-Dimensional Numerical Simulation of the Melting Temperature Field of the Cement-Improved Soil Cup-Shaped Permafrost wall. *Coalfield Geology. Exploration* 45 (04), 102–106. doi:10.3969/j.issn.1001-1986.2017.04.018

Wang, X. Y., Song, Q. Y., and Gong, H. (2022a). Research on Deformation Law of Deep Foundation Pit of Station in Core Region of Saturated Soft Loess Based on Monitoring. *Adv. Civil Eng.* 2022, 1–16. doi:10.1155/2022/7848152

Wang, X. Y., Ma, Z., and Zhang, Y. T. (2022b). Research on Safety Early Warning Standard of Large-Scale Underground Utility Tunnel in Ground Fissure Active Period. *Front. Earth Sci.* 10, 9. doi:10.3389/feart.2022.828477

Wu, Y. J., Yang, M., and Li, D. Y. (2006). Numerical Analysis of Freezing Soil Curtain of Tunnel Connected Aisle. *Rock Soil Mech.* 27 (3), 487–490. doi:10.16285/j.rsm.2006.03.033

Xu, X. M. (2018). Improved Design of Shield Receiving Steel Sleeve.Construction Mechanization. *Mod. transportation Technol.* 356 (09), 2426. doi:10.13311/j.cnki.conmec.2018.09.006

Yan, H., Wang, T. L., and Liu, J. K. (2013). Experimental Study of Repeated Frost Heave and Thaw Settlement Properties of Silty Sand. *Rock Soil Mech.* 34 (11), 3159–3165. (in Chinese). doi:10.16285/j.rsm.2013.11.012

Yang, P., Chen, J., and Zhang, S. G. (2017). Research on Full-Scale Measurement of Construction Temperature and Displacement Field of the Freezing Method for the Connection Channel in Weak Stratum. *Chin. J. Geotechnical Eng.* 39 (12), 2226–2234. doi:10.11779/CJGE201712011

Yuan, Y. H., Yang, P., and Jiang, T. Q. (2010). Study of thermal Field of Soil Freezing in Shallow Covered Tunnel with Subsurface Excavation Passing through Ground with Thin Aquifer under Complex Conduction. *Rock Soil Mech.* 31 (S1), 388–393. doi:10.16285/j.rsm.2010.s1.025

Zhao, L. F. (2013). Receiving Technology of Earth Pressure Balanced Shield Reaching Steel Sleeve Assisted Construction. *Railway Stand. Des.* 619 (08), 89–93. doi:10.13238/j.issn.1004-2954.2013.08.032

Zhao, L., Yang, P., Liu, Z. G., Yao, M. W., and Chen, L. (2017). Cup-Shaped Horizontal Freezing Method End Reinforcement and Steel Sleeve-Assisted Shield Receiving Technology. *Urban Rail Transit. Res.* 20 (09), 126–130. doi:10.16037/j.1007-869x.2017.09.026

Zheng, L. F., Gao, Y. T., and Zhou, Y. (2020). Research on Surface Frost Heaving and Thawing Settlement and Optimization of Frozen Wall Thickness in Shallow Buried Tunnel Freezing Method. *Geotechnical Mech.* 316 (06), 2110–2121. doi:10.16285/j.rsm.2019.1102

Conflict of Interest: CT and JZ were employed by China Railway Seventh Bureau Group Third Engineering Co., Ltd.

The authors declare that the research was conducted in the absence of any commercial or financial relationships that could be construed as a potential conflict of interest.

Publisher's Note: All claims expressed in this article are solely those of the authors and do not necessarily represent those of their affiliated organizations, or those of the publisher, the editors and the reviewers. Any product that may be evaluated in this article, or claim that may be made by its manufacturer, is not guaranteed or endorsed by the publisher.